BOND AND FLEXURAL BEHAVIOR OF CONCRETE ELEMENTS STRENGTHENED WITH NSM CFRP LAMINATE STRIPS UNDER FATIGUE LOADING

Pedro M. G. Fernandes[1], Patrícia M. Silva[2], José Sena-Cruz[3]*

ISISE, University of Minho, Department of Civil Engineering, Guimarães, Portugal

Abstract: This paper presents the results of an experimental research on bond and flexural behavior of concrete elements strengthened with carbon fiber reinforced polymer (CFRP) laminate strips under fatigue loading conditions, applied according to the near-surface mounted (NSM) strengthening technique. Long-term performance of the NSM system could be compromised by fatigue loading, which may result in deterioration and weakening of individual components (steel, FRP, concrete), or loss of bond performance and composite action. Hence, an experimental program composed of direct pullout tests and slab specimens was carried out to evaluate the influence of the stress level and amplitude of cycles imposed to the specimens. In bond fatigue tests, debonding failure occurred for a maximum stress level corresponding to 60% of the ultimate bond load obtained from monotonic loading. The fatigue loading imposed on the slabs did not yield to its failure. Consequently, the load carrying capacity obtained from post-fatigue tests of strengthened slabs was not significantly affected by this action.

Keywords: Fatigue, Bond and flexural behavior, Near-surface mounted (NSM), Carbon fiber reinforced polymer (CFRP), Stress level.

[1] PhD Student, ISISE, University of Minho, Department of Civil Engineering, Azurém 4800-058 Guimarães, Portugal. E-mail: pfernandes@civil.uminho.pt
[2] PhD Student, ISISE, University of Minho, Department of Civil Engineering, Azurém 4800-058 Guimarães, Portugal. E-mail: patricia.silva@civil.uminho.pt
[3] Associate Professor, ISISE, University of Minho, Department of Civil Engineering, Azurém 4800-058 Guimarães, Portugal. E-mail: jsena@civil.uminho.pt *Corresponding Author

1 INTRODUCTION

During the last few years, the near-surface mounted (NSM) strengthening technique using fiber reinforced polymers (FRP) has been adopted to increase the load carrying capacity of concrete members. Up to now, the research has been mainly focused on structural aspects, such as: bond behavior, flexural and/or shear strengthening effectiveness, and energy dissipation capacity of beam-column joints [1]. Contrarily, some other key issues, like durability and long-term performance of the NSM technique still deserve many research efforts.

In the context of strengthening of reinforced concrete (RC) structures, FRP applications have increasingly emerged to extend the service life of existing transportation infrastructures, such as bridges. This type of structures is subject to fatigue loading caused by fluctuating cycles of vehicle loads with different intensities. Repeated or cyclic loading, which is a typical load condition in bridges, present a significant influence on the FRP-concrete interface properties, as it is described in recent literature [2]. Although typical repeated or cyclic loading ranges are considerably lower than the ultimate carrying capacity of the structures, they can cause the failure by fatigue [3].

The experimental research on fatigue of strengthened structures with NSM system is scarce. Yost et al. [4] studied the behavior of simply supported reinforced concrete beams strengthened in flexure with NSM carbon fiber reinforced polymer (CFRP) bars and strips under fatigue loading. The beams were loaded under force control, between a minimum stress level (S_{min}) of 5% and maximum stress level (S_{max}) of 32%, and 2 million cycles were imposed at a frequency of 2.5 Hz. The beams did not fail by fatigue loading. Then, they were monotonically tested up to the failure. All the beams exhibited the same failure mode: yielding of the steel reinforcement followed by concrete crushing. From obtained results no significant changes were observed in the beams submitted to fatigue loading when compared with the control beams. Sena-Cruz et al. [5] also developed an experimental study by strengthening beams with CFRP laminates according to NSM technique and subjecting them to one million cycles. The fatigue tests were performed between S_{min}=25% and S_{max}=55%. Again, the beams did not fail by fatigue loading. The post-fatigue test revealed a marginal increase in terms of ultimate load, when compared with the control beam (not submitted to fatigue loading).

Several researchers have been also studying the fatigue behavior of RC beams strengthened with prestressed or non-prestressed CFRP rods [6-8]. According to Badawi et al. [8], the strengthened beams with NSM CFRP rods showed a longer fatigue life than those of the unstrengthened beam, at a given load range. The strengthening beam with NSM CFRP rods increased the fatigue life by five times with respect to the control beam, primarily at higher load ranges. In the same experimental study, the failure mode observed in the NSM

CFRP strengthened and unstrengthened beams was fatigue failure in the tension steel reinforcement. Rosenboom et al. [6] carried out experimental tests in which prestressed concrete bridge girders with NSM CFRP rods and laminates subjected to fatigue loading are compared. Both girders exhibited a higher stiffness and displacements degradation during the first 10,000 cycles. The displacements degradation after the initial cycles was very small and the girder stiffness remained constant up to 2 million cycles. The authors concluded that the incremental increase of the deflection is primarily due to the fatigue creep of the concrete in the compression zone.

In the context of study of bond behavior, the majority of the existing research about FRP bond systems under fatigue loading was performed with externally bonded reinforcement (EBR) [3]. Hence, the existing knowledge on the NSM-FRP bond systems under fatigue loading is much more limited. Yun et al. [3] studied and compared the bond behavior between FRP materials and concrete for different strengthening techniques under fatigue loading. The investigated strengthening techniques and FRP bond systems include NSM, EBR, fiber anchored (FB-FRP) and hybrid bonded FRP system (HB-FRP), through double shear bond test. Two million cycles were imposed at 5 Hz of frequency. From the obtained results, the authors concluded that the specimens strengthened with NSM-FRP systems, under fatigue loading, yielded to higher elastic and residual slips than the ones obtained from the other systems. In terms of bond stiffness, lower values were observed for the specimens strengthened with NSM-FRP systems. The authors of these tests also concluded that the slip increased much faster in the earlier cycles, than in the later cycles. The peak load of the monotonic post-fatigue tests was not affected by the fatigue load amplitude. The slope of the load-slip response after fatigue loading was influenced by the fatigue load level. In fact, increasing the fatigue load level, a reduction in post-fatigue bond stiffness was verified.[3].

To study the bond and flexural behavior of concrete elements strengthened with NSM-CFRP systems under fatigue loading conditions, an experimental program composed of direct pullout tests and slab specimens was carried out, respectively. The influence of fatigue level and cycle amplitude on the global response of the system was investigated. The results are presented and carefully analyzed in the following sections.

2 EXPERIMENTAL PROGRAM

The experimental study addressed an investigation on bond and flexural behavior of concrete elements strengthened with NSM-CFRP laminate strips under fatigue loading, composed of nine direct pullout tests (DPT) and six slab specimens (SL).

The fatigue response of FRP-strengthened concrete elements depends on the fatigue limits imposed (range of the applied load) [2, 9]. Usually, the minimum and maximum load of a fatigue cycle, F_{min} and F_{max}, respectively, to be applied to a specimen, are defined as a percentage of the maximum load carrying capacity, F_p, of the control specimen tested up the failure under monotonic static loading. Additionally, the minimum fatigue level S_{min} (=F_{min}/F_p), and maximum fatigue level, S_{max} (=F_{max}/F_p), the fatigue ratio, R (=S_{min}/S_{max}), as well as the number of cycles that the specimen was submitted, N_c are also defined.

Table 1 presents all the specimens included in the experimental program divided in five series. The code names given to the specimens consist on alphanumeric characters separated by underscores. The first string designates the specimen type (DPT – direct pullout test specimen, SL – slab specimen). In the case of the DPT, the second string specifies the specimen number (1, 2 and 3), while for the slabs indicates if it is strengthened (STR) or not (UN). The third string defines the load type (M – monotonic load, F – fatigue load). Finally, for the case of fatigue tests, the last character gives the value of applied S_{max} (50, 60, 70, 75 and 80).

The fatigue limits adopted in pullout tests were based on the results obtained from the monotonic tests performed before the fatigue ones. The minimum and maximum fatigue load levels adopted in pullout bond tests were selected with the objective to lead to the failure of the specimens by fatigue. In this context, preliminaries tests were performed by the authors in order to evaluate the load level for which the failure may occur. For the case of the slabs specimens, the fatigue study was focused on the three main regions observed in the monotonic test response, namely: (i) after cracking and before yielding load; (ii) after yielding load; and, (iii) between (i) and (ii).

2.1 Specimens and test configuration

2.1.1 Pullout specimens

Figure 1 shows the specimen geometry and test configuration adopted for the monotonic and fatigue direct pullout tests (DPT). The specimen geometry consisted of concrete cubic blocks of 200 mm of edge, in which a CFRP laminate strip with 1.4 mm of thickness and 10 mm of width is embedded. The groove with a rectangular cross-section of 15×5 mm^2 was cut with a saw cut machine.

According to previous experimental programs [10] the effective length of the strengthening system configuration adopted in the present work is in the range of 80 mm to 90 mm, being FRP rupture the failure mode to be observed. In this context a constant bond length of 60 mm was adopted, based on the following considerations: (i) the bond length must be large enough to be representative of the system and to make

negligible the unavoidable end effects; (ii) the bond length should avoid the failure of the FRP reinforcement; (iii) the bond length should be higher than the average crack spacing observed in the strengthened slabs (equal to 34 mm for the present case).

To avoid premature splitting in the concrete ahead the loaded end, a 100 mm unbonded length was left from the top of the block. A steel plate with 20 mm of thickness was placed at the top of the concrete block to assure negligible vertical displacements at the top of the concrete specimen during pullout test. This plate was fixed to the stiff base through four M10 steel threaded rods. A torque of 30 N×m was applied to fasten these rods, inducing an initial compression state on concrete block of about 2.0 MPa.

The instrumentation of the monotonic and fatigue DPT consisted of two linear variable differential transducers (LVDTs), as shown in **Figure 1**, and a load cell. LVDT1 (range ±5 mm with linearity error of ±0.09% F.S.) recorded the relative displacement between concrete and the CFRP laminate at the top of the concrete block (100 mm apart from the loaded end section), while the LVDT2 (range ±1 mm with linearity error of ±0.05% F.S.) was used to measure the slip at the loaded-end, s_l. The applied load, F, was registered by a load cell placed between the grip and the actuator, with a static load carrying capacity of 200 kN (linearity error of < ±0.05% F.S.).

The monotonic tests were performed under displacement control, with a rate of 2 μm/s, by using a LVDT placed between the actuator and the grip. Each fatigue test comprises the following three main steps: (i) the specimen was initially pre-loaded under force control at a load rate of 64 N/s up to $(F_{max} + F_{min})/2$; (ii) then a sinusoidal load characterized by an amplitude of $(F_{max} - F_{min})/2$ and a frequency of at 3 Hz was imposed (up to 3 million cycles); (iii) the specimens that did not fail during the fatigue loading were monotonically tested up to the failure with the same configuration of the monotonic tests (post-fatigue test). Finally, it should be remarked that the adopted frequency took into account the maximum amplitude allowed by servo-controlled equipment used.

2.1.2 Slabs specimens

The slabs geometry and reinforcement detailing are presented in **Figure 2**. The slabs geometry are 2000 mm long, 300 mm wide and 80 mm thick. The longitudinal reinforcement is composed by 4Ø6, which corresponds to a longitudinal reinforcement ratio, ρ_l, equal to 0.47%. The flexural strengthening solution is composed by 3 CFRP laminate strips and was introduced according to NSM technique in the uncracked stage of the slabs. The

corresponding equivalent longitudinal reinforcement ratio [5] $\rho_{s,eq}$ is 0.68%. In this experimental study, a four-point bending test configuration was adopted for monotonic and fatigue tests (see **Figure 2c**). In both tests the instrumentation of the slab included LVDTs, load cell (the same one used for the direct pullout tests) and strain gauges (TML BFLA-5-3-3L for measuring the strains in CFRP and steel; TML PFL-30-11-3L for measuring the strains in concrete). Five LVDTs measured the deflection along the slab's longitudinal axis (see **Figure 2c**), whereas the load cell recorded the applied vertical force. In order to measure the strains in distinct sections, five strain gauges (SG1 to SG5) were glued on the lateral surface of the intermediate CFRP laminate strip. Additionally, two strain gauges (SG6 and SG7 in **Figure 2b**) were used to record the strains in the longitudinal steel reinforcement and one on concrete at the top fiber of the cross-section midspan.

The fatigue tests were composed by three main steps: initially, in order to obtain the initial response of the slab, a monotonic loading was applied under force control at a load rate of 100N/s up to the maximum level (S_{max}); then, 2 million cycles were imposed at 2 Hz of frequency between F_{min} and F_{max}; finally, in case that the 2 million cycles did not lead the specimens to failure, a monotonic loading was applied to the slabs up to failure. The adopted frequency took into account the maximum amplitude allowed by servo-controlled equipment used. In the monotonic tests, the internal displacement transducer of the servo-control equipment was used to control the test at 20 μm/s of deflection rate.

2.2 Materials characterization

2.2.1 Concrete

Only one batch was used to cast all the specimens (slabs, blocks for the DPT and cylinders for the concrete mechanical characterization). The mechanical characterization of the concrete was assessed by means of compression tests. Five cylindrical concrete specimens with 150 mm of diameter and 300 mm height were tested at 28-days of concrete age to evaluate the modulus of elasticity and the compressive strength according to, respectively, LNEC E397-1993:1993 and NP EN 12390-3:2011 recommendations [11, 12]. The results obtained in the compression tests indicated an average compressive strength value of 36.0 MPa, with a coefficient of variation (CoV) of 3.9%, and an average Young's modulus of 28.4 GPa (CoV=5.8%). At the time of the fatigue tests, the average concrete compressive strength in cylinders was 48.2 MPa (CoV=3.2%). The age of the concrete at the date of experimental program was about one year for the slab specimens and one and a half year for pullout bond specimens.

2.2.2 Steel reinforcement

The grade of the steel longitudinal reinforcement is A500 NR, according to [13]. Tensile tests were performed to assess the mechanical characteristics of the steel reinforcement (Ø6), in accordance to NP EN 10002-1:1990 [14]. From these tests, the obtained average values of E-modulus, hardening modulus and ultimate strength were, respectively, 212.2 GPa (CoV=6.3%), 0.7 GPa (CoV=6.6%) and 733.0 MPa (CoV=1.0%).

2.2.3 CFRP laminate strips

The CFRP laminate strips used in the present experimental work are produced by S&P® Clever Reinforcement Company. The laminate has the trademark CFK 150/2000 and is composed of unidirectional carbon fibers agglutinated by an epoxy vinylester resin. This laminate has a rectangular cross-section of 10×1.4 mm^2 and the external surface is smooth. Young's modulus and tensile strength evaluation of the CFRP laminate were performed according to ISO 527-5:1997 [15]. From six tested specimens, a Young's modulus, a tensile strength and a strain at peak stress of 169.5 GPa (CoV=2.5%), 2648.3 MPa (CoV=1.8%) and 1.6% (CoV=1.8%) were obtained, respectively.

2.2.4 Epoxy adhesive

The S&P Resin 220 epoxy adhesive®, produced by the same supplier of the CFRP material, was used to bond the laminate strips to the concrete. This epoxy adhesive is a solvent free, thixotropic and grey two-component (Component A = resin and Component B = hardener). To assess the mechanical properties of the hardened adhesive, tensile tests were carried out according to the ISO 527-2:2012 [16]. After casting, five specimens were cured and kept in the lab environment during five months before being tested. From the tests an average tensile strength of 22 MPa (CoV=4.52%), Young's modulus of 7.15 GPa (CoV=3.71%) and a strain at the peak stress of 0.36 MPa (CoV=15.22%) were obtained.

2.3 Preparation of the specimens

The preparation of the strengthened specimens required several steps, mainly: (i) opening the grooves with a saw cut machine (ii) cleaning the grooves with compressed air and the CFRP laminates with acetone; (iii) preparation of the adhesive according to the technical data sheet; (iv) application of the adhesive on the groove and lateral surfaces of the laminate; (v) introducing carefully the laminate into the groove; (vi) level the surface. After opening the grooves, several measurements were carried out to assess the actual grooves geometry. These

measurements indicated average values of width and depth of 5.61 mm (CoV=1.91%) and 15.70 mm (CoV=1.94%) for pullout specimens, respectively. For the case of slabs the width was 5.47 mm (CoV=1.82%) and the depth was 15.59 mm (CoV=2.16%). The strengthening of the specimens was carried out at about 95 days after casting concrete. At that moment, the opened grooves were completely dry and clean. The strengthening was performed in the interior of the lab with an average temperature of about 25ºC and 42% of relative humidity. The specimens were kept in laboratory environment until they were tested.

3 RESULTS AND DISCUSSION

3.1 Monotonic tests

3.1.1 Pullout specimens

Table 2 summarizes the main results obtained in monotonic pullout tests (series S1). In this table the meaning of each entity is the following: $F_{f\max}$ is the maximum pullout force; F_{fu} is the CFRP tensile strength; $s_{l\max}$ is the slip at the loaded end at $F_{f\max}$; $\tau_{\max,av}$ is the average bond strength at the CFRP-epoxy interface and is evaluated by $F_{f\max}/(P_f L_b)$ where P_f (= $2 \times w_f + 2 \times t_f$) is the perimeter of the CFRP cross-section in contact with the adhesive, being w_f and t_f the width and the thickness of the CFRP and L_b is the bond length. In general, the parameters presented quite low values of the corresponding coefficients of variation. It is also remarkable, that the adopted bond length (60 mm) explored at about 82% of the ultimate carrying capacity of the CFRP laminate.

Figure 3 depicts the envelope of pullout force *versus* loaded end slip (F_l-s_l) relationship for all three specimens tested monotonically up to the failure (DPT_M). The relationship F_l-s_l is eminently non-linear from the origin to the peak load. This response can be justified by the non-linear behavior of the adhesive and, when the chemical bond between the concrete/adhesive and adhesive/CFRP starts being damaged, the debonding process begins. It can also be observed a short post-peak descending branch, justified by the failure mode observed, i.e. debonding failure at the adhesive/laminate interface. This failure mode was expected, since the concrete groove surface is rougher than the external surface of the CFRP laminate.

3.1.2 Slab specimens

As previously referred, two slabs were initially subjected to monotonic tests up to the failure: one unstrengthened slab (SL_UN_M), and another one strengthened (SL_STR_M), in order to (i) define the stress levels to apply in the fatigue tests and (ii) compare their performance the ones obtained in the fatigue testes. The results obtained in these tests are presented in **Table 3** showing the following parameters: midspan deflection and applied load

for crack initiation (δ_{cr}, F_{cr}), yield initiation of the longitudinal reinforcements (δ_y, F_y), maximum load (δ_{max}, F_p), and failure mode. **Figure 4** presents the relationship between the applied load (F) and the midspan deflection (δ) for both slabs. In the F-δ curves are clearly identified three branches corresponding to the three stages with distinct slopes, namely: stage I – uncracked concrete; stage II – cracked concrete; stage III – cracked concrete with the steel reinforcement yielded.

Figure 5 shows the evolution of steel strain with the applied load. From this chart it is possible to observe that yielding initiation occurred at about 0.36% and 0.38% for the SL_UN_M and SL_STR_M slabs, respectively. These values are quite close to the expected one (about 0.33% – *c.f.* 2.2.2). At the maximum load the registered concrete strain in the SL_UN_M and SL_STR_M slabs was of about 0.38% and 0.48%, respectively. These high concrete strain values were expected since both specimens failed by concrete crushing (CC) at the top part of the slab in the midspan region. It is also noticeable that the level of strengthening efficiency was quite high. As can be seen in **Table 3**, the CFRP strains reached 1.2%, which is a common value in NSM systems and twice higher than the reported for the EBR technique [17]. The stiffness variations from stage I to II and II to III for the REF slab were -87% and -92%, respectively, while in the STR slab were -84% and -56%. The smaller variation observed for the STR slab from stage II to III was expected since, after yielding initiation of the longitudinal reinforcement, the CFRP laminate is responsible for the increase of the load carrying capacity.

The average bond stress between two consecutive strain gauges *i* and *j*, τ_m^{ij}, was also evaluated by using the following equation:

$$\tau_m^{ij} = \frac{E_f \cdot A_f \cdot \Delta\varepsilon_f^{ij}}{P_f \cdot L^{ij}} \tag{1}$$

where E_f and A_f are the Young's modulus and the cross-sectional area of the CFRP; P_f is the perimeter of the contact surface between FRP and adhesive; L^{ij} is the distance between two consecutive strain gauges; and, $\Delta\varepsilon_f^{ij}$ is the axial strain variation of strain gauges positioned at *i* and *j* sections.

Figure 6 presents the relationship between the total load and the average bond stress at SG3-4 (see also **Figure 2b**), where a gradual evolution of the bond stresses is observed along the tests. At the ultimate load (F_p), the average bond stress had the approximate value of 3 MPa for the slab SL_STR_M.

Finally, the crack spacing of the REF and STR slabs were assessed. An average value at about 80 mm and 34 mm was obtained for the REF and STR, respectively, highlighting the greater capacity of the strengthened system in having a better distribution of the cracks in the RC specimen.

3.2 Fatigue tests

3.2.1 Pullout specimens

As previously mentioned, six pullout specimens were tested under two different fatigue load ranges: (i) 23%-52% (series S2), and (ii) 26%-58% (series S3) of the average maximum pullout force, $F_{f\max}$, obtained from the three specimens tested under monotonic loading (see also **Table 1**).

Figure 7 shows typical pullout force *versus* loaded end slip responses during fatigue tests (specimens DPT2_F50 and DPT2_F60). For the three fatigue tests of series S3, the number of cycles at failure (N_f) were 95,000, 561,000 and 376,000 cycles for the specimens DPT1_F60, DPT2_F60 and DPT3_F60, respectively. Even though these specimens were submitted to the same fatigue and amplitude load, they presented a significant scattering behavior in terms of their number of cycles at failure. Nevertheless, the failure mode observed in these three specimens was identical and corresponded to progressive debonding of the CFRP at adhesive/laminate interface up to a complete separation between both materials. From **Figure 7** it can be observed that the hysteresis curves of all tested pullout specimens presented similar shape along the fatigue cycles. For any given cycle, the load-slip curves exhibit an ascending branch and a descending branch that practically closes the hysteresis loops [3, 18]. The area enclosed by each loop represents the energy dissipated in that cycle [2, 9] and, for the S2 series, increased gradually with the number of cycles. The increase of the dissipated energy with the number of cycles has been also reported and observed by the other researchers e.g. [2, 3, 19] and it is a consequence of the bond deterioration caused by fatigue cycles [3]. In this S3 series a decrease in the dissipated energy was found for the last cycles (see **Figure 7b**). A justification for this aspect is given in the following paragraphs.

The evolution of loaded end slip (s_l) with respect to number of cycles are plotted in **Figure 8** for both maximum and minimum loads applied during the fatigue tests of series S2 and S3. The evolution of s_l with the number of cycles for the S2 series is composed of two regions: (i) a region of fast increase of the slip in the first cycles, followed by (ii) a progressive slip growth zone. On the other hand, for the three specimens of series S3, three regions can be identified: (i) a region of fast increase of the slip in the first cycles, followed by (ii) a progressive slip growth zone, like in the S2 series and finally (iii) a region where the slip increased faster again

until the specimen reached failure. The magnitude of values of the slip at the failure is in agreement with the ones obtained in monotonic tests, i.e. approximately 0.60 mm (see also **Figure 3**). In series S2, after a similar initial behavior (when compared with S3 series), the slip rate increase was much lower in the second stage. In this series, the specimens did not fail after being submitted to a 3 million of cycles and the maximum slip observed was approximately 0.30 mm in all three specimens. According to Yun et al. [3] the rate of increase in slip after 0.1 million cycles is considerably lower than the initial rate. This fact is verified in the present work and it was also observed by other researchers e.g. [18, 20, 21].

Figure 9 presents the evolution of the stiffness with the number of cycles. The stiffness was calculated as the slope of the line defined by the two points of F_l-s_l curve of **Figure 7**, corresponding to minimum and maximum pullout force in each cycle. In all specimens of series S2, the slopes of the cycles were found to be continuously decreased with the number of cycles, indicating a progressive and continuous loss (degradation) in terms of bond stiffness. For series S3, the same evolution in terms of stiffness was verified, except in the last cycles, in which, before the specimens failed, a slight increase in the stiffness occurred.

As shown in **Table 1**, the stress levels adopted for both series S2 and S3 were quite close. In spite of that, fatigue failure was only observed in the S3 series. In order to clarify this different behavior, the local bond stress-slip relationship $\tau - s$ was assessed by applying an analytical-numerical strategy [22], based on the experimental results obtained in series S1. Assuming that the CFRP laminate has a linear elastic behavior in its longitudinal direction and neglecting the concrete deformability in the slip determination, the second order differential equation that governs the local bond phenomena of the laminate-concrete interface is given by [22]:

$$\frac{d^2 s}{dx^2} = \frac{P_f}{E_f A_f} \cdot \tau(x) \tag{2}$$

where $\tau(x) = \tau\left[s(x)\right]$ is the local bond shear stress acting on the contact surface between the laminate and the concrete along the embedded length and s is the slip; the origin of x axis coincides with the free extremity of the bond length; the meaning of P_f, E_f and A_f, can be found in section 3.1. In the present study the following local bond stress slip law was assumed:

$$\tau(s) = \begin{cases} \tau_m \left(\frac{s}{s_m}\right)^{\alpha} & \text{if } s \le s_m \\ \tau_m \left(\frac{s}{s_m}\right)^{-\alpha'} & \text{if } s > s_m \end{cases} \tag{3}$$

Detailed description about the analytical model, as well as the inverse analysis strategy can be found elsewhere [22, 23]. Based on the inverse analysis performed τ_m=23.2 MPa, s_m=0.20 mm, α=0.18 and α'=0.11.

The F_l-s_l analytical-numerical response calibrated from S1 average experimental F_l-s_l curve is plotted in **Figure 3**. It is possible to observe that the numerical strategy used was able to predict the F_l-s_l response with good accuracy. **Figure 10** depicts the local bond stress, τ, evolution over the CFRP longitudinal embedded length (x) corresponding to an applied load of 50%, 60% and 100% of F_{fmax}. It can be observed, for the 50% and 60% levels, that only part of the bond length is mobilized and the $\tau - s$ is still in the ascending phase, remaining the rest of the bond length "virgin" or undamaged. For the 100% level of maximum pullout force it can be seen that about 73% of the bonded length is already in the descending branch of the $\tau - s$ curve (softening phase). Based on this simulation, it can be concluded that for an applied load of 50% (S2) and 60% (S3) of F_{fmax}, 74.3% and 84.4% of the total bond length is effective, respectively. During the fatigue test, as the effective bond length (closer to the loaded end) is becoming damaged by the fatigue cycles, the stresses shifted to the undamaged zone of the total bonded length (closer to the free end) thus allowing the stiffness to grow (see **Figure 9**). Although the stress transfer process occurred in an identical way for both series (S2 and S3), since the applied stress level in series S3 was higher than in S2, it probably led to a faster bond degradation and, consequently, to the corresponding failure.

Finally, the residual slip at the end of the fatigue tests of S2 series (unloaded specimens) were 0.08 mm, 0.09 mm and 0.006 mm for the specimens DPT1_F50, DPT2_F50 and DPT3_F50, respectively.

Post-fatigue monotonic behavior

As previously referred, specimens of S2 series did not fail by fatigue cycles. Thus, these specimens were loaded monotonically up to failure. The post-fatigue F_l-s_l monotonic responses are presented in **Figure 3**. **Table 2** also includes the relevant results obtained in the post-fatigue monotonic pullout tests of series S2. It should be remarked that the residual slip referred in the previous section was not added to the present results.

In general, with exception of the reduction in terms of initial bond stiffness, the overall bond behavior was not much affected by the stress level applied in the S2 series. As it can be seen in **Figure 3**, the F_l-s_l responses of S1 and S2 series differ until the maximum pullout force is achieved. In the tests which experienced fatigue load, three different regions can be identified. Region I (F_l less than 4.5 kN) has a lower stiffness than that observed in the monotonic tests due to the damage caused by the fatigue cycles in the effective bonded length. Contrarily, region III (F_l greater than 12.5 kN) presents a stiffness identical to the one observed in the

monotonic tests since this load level mobilizes undamaged regions of the system CFRP-adhesive-concrete. The remaining region II is a transition region between region I and III.

In comparison to series S1, the maximum pullout force had a slight decrease of about 6% and the loaded end slip was not influenced by the fatigue loading. The bond strength had a slight decrease due to fatigue action (see values of $\tau_{max,av}$ for series S1 and S2).

Figure 11 shows the failure modes occurred in monotonic and fatigue tests. In both monotonic and fatigue tests the failure mode in all specimens was very sudden and brittle, corresponding to debonding at the adhesive/laminate interface. For the specimens failed by fatigue action (series S3), it is possible to observe a small "wedge of adhesive" attached to the CFRP laminate and a thin adhesive layer glued on CFRP surface.

3.2.2 Slabs specimens

As previously reported, four fatigue tests were carried out with three strengthened and one unstrengthened slabs. All the fatigue tests included an initial monotonic loading phase up to the F_{max} (see **Table 1**) in order to register the initial response of each slab. **Table 3** presents some important results in terms of forces and corresponding deflections. In general, all the tested specimens exhibited a similar response to the corresponding reference ones (SL_UN_M and SL_STR_M).

After this initial phase, the slabs were then submitted to 2 million of cycles of sinusoidal load (*cf.* 2.1.2). Due to some technical problems in the servo-control equipment (overheating of the system) the tests of the slabs SL_STR_F70 and SL_STR_F80 were interrupted and restarted during the fatigue cycles phase. Because of that, the imposed force slightly changed (the maximum variation was about 11%).

Table 4 presents the results obtained in terms of midspan deflection (δ) due to the fatigue loading. In general a small increase in terms of δ was observed for all the slabs, including the unstrengthened one, as can be seen in **Figure 12**. The observed drops are due to technical problems faced in the actuator, as previously mentioned. In spite of that, the increase of deflection as result of fatigue is observed.

The deflection increase observed in all the strengthened slabs may be attributed to the bond degradation in steel-concrete and CFRP-concrete interfaces, as well as to progressive accumulation of plastic strains in the reinforcement (slabs SL_STR_F70 and SL_STR_F80), wedging of debris in flexural cracks, and also plastic deformation in the concrete. As expected, with the increase of F_{max}, the deflection at midspan also increased. However, in all tested slabs, higher variation of deflection (from the first cycle to the last one) was observed for the load level S_{min}, when compared to S_{max}. This behavior can be justified by the fact that, for the lower stress

level (S_{min}), the deflection is more dependent on the level of crack width, aggregate interlock and bond in the materials interfaces than the $S_{max.}$

During the fatigue cycles the evolution of the stiffness (K) of the slabs was also evaluated. This stiffness was calculated as the slope of the line defined between the lower and the upper points of the load–deflection curve of a complete cycle. In general, a marginal variation of K was observed when the first and last (2,000,000) fatigue cycles are compared, as shown in **Table 4**. As expected, the unstrengthened slab presented the highest stiffness degradation (5.7%). The **Figure 13** shows a typical relationship between the total load and the midspan deflection, where it can be seen a slight decrease of stiffness due to fatigue action. The highest decrease of stiffness occurred mainly in the first cycles.

Table 5 includes for each strengthened slab the strain variations at the midspan section between the first and last cycle for S_{min} and S_{max}. This table does not include the results of slab SL_UN_F75 because the strain gauge for measuring the concrete strains was damaged during the test. In general, CFRP, steel and concrete strains increase with S_{max}, as would be expected. Moreover, all strengthened slabs presented a marginal increase in CFRP strain, as shown in the **Figure 14**. In this figure it is also possible to observe some drops in the CFRP strain (especially for the case of SL_STR_F70), due to the technical problems faced in servo-control equipment (previously referred). Similar conclusions can be made from **Figure 15**, where the CFRP strain evolution for the slab SL_STR_F70 is plotted, and a slight variation is observed. Conversely, a significant increase in the concrete strain on the top fiber between the first and last cycle was observed. The main increase of the concrete strains of strengthened slabs register during the fatigue cycles was until to 500,000 cycles. Then, the concrete strains remained constant. Badawi et al. [8] also reported in strengthened beams with CFRP rods, an increase in the concrete compressive strains at an early stage of the loading, possibly due to concrete softening and creep due cyclic loading. According to the bibliography, repeated loads cause an increase in concrete creep when compared to creep under a constant sustained load. Thus, the increase in creep due to cyclic action is frequently designated cyclic creep [24, 25]. This phenomenon on concrete may justify the observed small increase of CFRP and steel strains in the present experimental program, additionally to the effects previously pointed out.

Comparing the CFRP stress level at the midspan of the slabs with the CFRP stress level observed in the F60 series of the pullout tests, the former was higher. In fact in the pullout tests that failed by fatigue, the CFRP laminate strips were submitted to a strain level at about as 0.75% (DPT_F60 series), while for the case of slab SL_STR_F80 (worst case), the measured CFRP strains ranged between 1.0% at the midspan and 0.12% at the extremities. In spite of that, the slabs did not fail by fatigue. Typically, direct pullout tests (DPT) are more

representative of the observed behavior at the ends of the FRP reinforcement of a flexural strengthened slabs, whereas beam pullout tests (BPT) better represent the behavior at the intermediate region to study for instance intermediate crack debonding, despite they have not been performed in these work. When BPT and DPT are compared, the former better represents the global behavior of the slabs, as can be seen in [26]. On the other hand, the high level of stress concentration occurred at the loaded end section in the DPT tests usually cannot be observed in structural elements.

Post-fatigue monotonic behavior

The post-fatigue monotonic behavior of all slabs is presented in **Figure 4**. As expected, for the tested slabs it is possible to observe an almost linear response up to the load corresponding to the maximum load level applied during the fatigue tests.

Figure 5 includes the response of the steel reinforcement for the post-fatigue tests, in which is possible to identify some similarity with the behavior observed in the F-δ curves. In general a higher stiffness is observed for the specimens that were submitted to the fatigue loading.

Comparing the slabs submitted to the post-fatigue monotonic tests with the corresponding control ones (SL_UN_M and SL_STR_M), an increase in terms of maximum force (F_p), as well as stiffness at the stabilized cracked stage (K_{II}) were observed. The load carrying capacity (F_p) increase for all strengthened slabs is about 9%, as shown in **Table 3**, due to the fact that cyclic load causes a re-arrangement of the dislocations density of the steel into a new configuration, inducing a significant hardening [27]. In this post-fatigue monotonic tests it is also possible to observe a decrease of the maximum deflections due to the residual deformation at the end of fatigue tests, that it has not been considered in the present table. The slab that was submitted to the lower maximum stress level (SL_STR_F50) presented highest stiffness in the stage II, of about 0.79 kN/mm. This value is approximately 42% higher than the one obtained in the slab SL_STR_M. The remaining strengthened slabs, SL_STR_F70 and SL_STR_S80 presented a stiffness (K_{II}) of 0.68 kN/mm (1.22 higher than SL_STR_M) and 0.62 kN/mm (1.11 higher than SL_STR_M), respectively. The increase of the K_{II} may be also justified by the hardening behavior of the steel reinforcement during the fatigue cycles. This better structural behavior, after applying fatigue cycles, it has been observed in previous research works, such as those reported by Yost et al. [4] and Sena-Cruz et al. [5].

The maximum CFRP strain is not affected by fatigue loading, since the measured maximum values were approximately equal to the ones observed in the reference tests. In general, the bond strength on the monitoring

region (see **Figure 6**) was not significantly modified by the fatigue cycles. Eventually, the main failure mode observed in all the slabs was concrete crushing at the top part of the slab in the midspan region (in between point loads).

4 CONCLUSIONS

This paper presented an experimental study on bond and flexural behavior of concrete elements strengthened with NSM CFRP laminate strips under fatigue loading, through direct pullout tests (DPT) and slab specimens (SL). A total of nine direct pullout specimens and six slab specimens were tested. From the bond pullout and slab tests, the following conclusions can be highlighted:

1. Debonding failure at adhesive/laminate interface up to complete separation occurred by fatigue loading for a maximum fatigue stress level (S_{max}) of about 60%. For a maximum fatigue stress level of about 50% the specimens did not fail after have been submitted to 3 million of cycles. Progressive and continuous loss degradation in terms of bond stiffness was observed, for both studied fatigue load levels;
2. The monotonic post-fatigue tests (series S2) show that, in terms of bond performance, the fatigue loading caused a significant reduction in the initial bond stiffness. However, in terms of maximum pullout force a slight decrease of 6% was verified;
3. Using an analytical-numerical approach, a local bond stress–slip relationship was assessed from the experimental test results. This strategy was useful to justify that during the fatigue testes the effective bond length observed in S2 series was lower than the one in S3 series at about 14%;
4. All the strengthened slabs submitted to fatigue cycles (specimens submitted to a maximum fatigue stress level of about 50%, 70% and 80%) presented a lower increase in terms of midspan deflection than the one observed in the unstrengthened slab at the end of the corresponding fatigue test. In general, the strains in the CFRP laminate and steel reinforcement marginally increased. The stiffness variation slightly changed during the fatigue cycles. The highest decrease rate of the stiffness occurred mainly in the first cycles. In spite of being submitted to 2 million of fatigue cycles, none of the slabs failed by fatigue;
5. The monotonic tests carried out after the fatigue cycles (post-fatigue tests) have shown slightly increase in terms of ultimate load and stiffness comparatively to the reference slabs. The main failure mode observed in all the slabs was concrete crushing at the top part of the slab in the midspan region (in between point loads). Therefore, from this study it can be concluded that the damage accumulation due the fatigue cycles neither affected the ultimate capacity of the strengthened NSM CFRP slabs, nor the failure mode.

In spite of the present results being credible and contributing for the knowledge in this area, further experimental work supported in analytical and numerical simulations, e.g. studies on the effect of the longitudinal and equivalent longitudinal reinforcement ratios, the effect of the concrete strength class and the effect frequency on the fatigue response, are needed to fully understand the global fatigue behavior of the NSM-CFRP systems and to confirm the observed tendencies.

ACKNOWLEDGEMENT

This work is supported by FEDER funds through the Operational Program for Competitiveness Factors - COMPETE and National Funds through FCT - Portuguese Foundation for Science and Technology under the project CutInDur PTDC/ECM/112396/2009. The authors also like to thank all the companies that have been involved supporting and contributing for the development of this study, mainly: S&P Clever Reinforcement Ibérica Lda., Casais – Engenharia & Construção S.A., Artecanter - Indústria de Transformação de Granitos, Lda., Tecnipor - Gomes & Taveira Lda., Vialam – Indústrias Metalúrgicas e Metalomecânicas, Lda., Hilti Portugal-Produtos e Serviços, Lda., Novo Modelo Europa, S.A., Sika Portugal - Produtos Construção e Indústria, and S.A., Cachapuz - Equipamentos para Pesagem, Lda. The first and second authors wishes also to acknowledge the grants SFRH/BD/80338/2011 and SFRH/BD/89768/2012, respectively, provided by FCT.

REFERENCES

[1] De Lorenzis L, Teng JG. Near-surface mounted FRP reinforcement: An emerging technique for strengthening structures. Composites Part B: Engineering 2007;38(2):119-143.

[2] Carloni C, Subramaniam KV. Investigation of sub-critical fatigue crack growth in FRP/concrete cohesive interface using digital image analysis. Composites Part B: Engineering 2013;51(6):35-43.

[3] Yun Y, Wu Y-F, Tang WC. Performance of FRP bonding systems under fatigue loading. Engineering Structures 2008;30(11):3129-3140.

[4] Yost JR, Gross SP, Deitch MJ. Fatigue behavior of concrete beams strengthened in flexure with near surface mounted CFRP. In: 8th international symposium on fiber reinforced polymer reinforcement for reinforced concrete structures (FRPRCS-8), Patras, Greece; 2007. p. 8.

[5] Sena-Cruz JM, Barros JAO, Coelho MRF, Silva LFFT. Efficiency of different techniques in flexural strengthening of RC beams under monotonic and fatigue loading. Construction and Building Materials 2012;29(24):175-182.

[6] Rosenboom O, Rizkalla S. Behavior of Prestressed Concrete Strengthened with Various CFRP Systems Subjected to Fatigue Loading. Journal of Composites for Construction 2006;10(6):492-502.

[7] Badawi M, Soudki K. Flexural strengthening of RC beams with prestressed NSM CFRP rods - Experimental and analytical investigation. Construction and Building Materials 2009;23(10):3292-3300.

[8] Badawi M, Soudki K. Fatigue Behavior of RC Beams Strengthened with NSM CFRP Rods. Journal of Composites for Construction 2009;13(5):415-421.

[9] Kim Y, Heffernan P. Fatigue Behavior of Externally Strengthened Concrete Beams with Fiber-Reinforced Polymers: State of the Art. Journal of Composites for Construction 2008;12(3):246-256.

[10] Costa IG, Barros JAO. Evaluation of the influence of the adhesive properties and geometry of carbon fiber laminates using pull-out tests. University of Minho, Report no. 12-DEC/E-08, Department of Civil Engineering, 2012. p. 16.

[11] LNEC, Concrete – Determination of the elasticity young modulus under compression, in *E397-1993*, ed: Portuguese specification from LNEC, 1993.

[12] NP, Testing hardened concrete. Part 3: Compressive strength of test specimens, in *EN 12390-3*, ed. Caparica: Instituto Português da Qualidade (IPQ), 2011.

[13] NP, Eurocode 2: Design of concrete structures - Part 1-1: General rules and rules for buildings, in *EN 1992-1-1*, ed. Brussels: European Committee for Standardization (CEN), 2010.

[14] NP, Metallic materials - Tensile testing. Part 1: Method of test (at ambient temperature), in *EN 10 002-1*, ed. Caparica: Instituto Português da Qualidade (IPQ), 1990, p. 34.

[15] ISO, Plastics - Determination of tensile properties - Part 5: Test conditions for unidirectional fibre-reinforced plastic composites, in *527-5*, ed. Genève, Switzerland: International Organization for Standardization (ISO), 1997, p. 11.

[16] ISO, Plastics – Determination of tensile properties – Part 2: Test conditions for moulding and extrusion plastics, in *527-2*, ed. Genève, Switzerland: International Organization for Standardization (ISO), 2012, p. 5.

[17] CNR-DT 200, Guide for the Design and Construction of Externally Bonded FRP Systems for Strengthening Existing Structures, in *CNR - Advisory Committee on Technical Recommendations for Construction, Italy, 154 pp, 2004*, ed, 2004.

[18] Gheorghiu C, Labossière P, Proulx J. Response of CFRP-strengthened beams under fatigue with different load amplitudes. Construction and Building Materials 2007;21(4):756-763.

[19] Carloni C, Subramaniam KV, Savoia M, Mazzotti C. Experimental determination of FRP–concrete cohesive interface properties under fatigue loading. Composite Structures 2012;94(4):1288-1296.

[20] Barnes R, Mays G. Fatigue Performance of Concrete Beams Strengthened with CFRP Plates. Journal of Composites for Construction 1999;3(2):63-72.

[21] Shahawy M, Beitelman T. Static and Fatigue Performance of RC Beams Strengthened with CFRP Laminates. Journal of Structural Engineering 1999;125(6):613-621.

[22] Sena-Cruz JM, Barros J. Modeling of bond between near-surface mounted CFRP laminate strips and concrete. Computers & Structures 2004;82(17–19):1513-1521.

[23] Sena-Cruz JM, Barros JAO, Gettu R, Azevedo FM. Bond behavior of near surface mounted CFRP laminate strips under monotonic and cyclic loading. Journal of Composites for Construction, ASCE 2006;10(4):295-303.

[24] Higgins L, Forth JP, Neville A, Jones R, Hodgson T. Behaviour of cracked reinforced concrete beams under repeated and sustained load types. Engineering Structures 2013;56(40):457-465.

[25] Whaley C, Neville A. Non-elastic deformation of concrete under cyclic compression. Magazine of Concrete Research 1973;25(84):145-154.

[26] Sena-Cruz J, Silva P, Fernandes P, Azenha M, Barros J, Sousa C, Castro F, Teixeira T. Creep behavior of concrete elements strengthened with NSM CFRP laminate strips under different environmental conditions. In: FRPRCS-11: 11th International Symposium on Fiber Reinforced Polymer for Reinforced Concrete Structures, Guimarães; 2013. p. 12.

[27] Hussain K, De Los Rios E. Monotonic and cyclic stress-strain behaviour of high strength steel. Metallurgical Science and Tecnology 1993;11(1):2-30.

List of Tables

Table 1 — Experimental program composed of direct pullout and slab tests.

Specimen type	Series	Specimen	F_p [kN]	F_{min} [kN]	F_{max} [kN]	S_{min} [%]	S_{max} [%]	R	N_C
Direct pullout tests	**S1**	DPT1_M	29.7	-	-	-	-	-	-
		DPT2_M	30.9	-	-	-	-	-	-
		DPT3_M	30.4	-	-	-	-	-	-
	S2	DPT1_F50	-	7.1	15.9	23	52	0.45	3,000,000
		DPT2_F50	-	7.0	15.8	23	52	0.44	3,000,000
		DPT3_F50	-	7.0	15.8	23	52	0.44	3,000,000
	S3	DPT1_F60	-	7.7	17.7	25	58	0.44	95,000
		DPT2_F60	-	7.8	17.9	26	59	0.43	561,000
		DPT3_F60	-	7.9	17.7	26	58	0.44	376,000
Slabs	**S4**	SL_UN_M	12.0	-	-	-	-	-	2,000,000
		SL_STR_M	31.6	-	-	-	-	-	2,000,000
	S5	SL_UN_F75	-	5.1	9.0	42	75	0.57	2,000,000
		SL_STR_F50	-	8.3	15.1	26	48	0.55	2,000,000
		SL_STR_F70	-	16.2	22.5	51	71	0.72	2,000,000
		SL_STR_F80	-	19.6	26.3	62	83	0.75	2,000,000

Table 2 — Main results obtained from the monotonic and post-fatigue monotonic pullout tests.

Specimen	F_{fmax} [kN]	F_{fmax} / F_{fu} [%]	$\tau_{max,av}$ [MPa]	s_{lmax} [mm]	**Failure mode**
DPT1_M	29.7	80.3	21.7	0.58	D
DPT2_M	30.9	83.6	22.6	0.59	D
DPT3_M	30.4	82.2	22.2	0.55	D
DPT_M	30.4* (1.99%)	82.0* (1.99%)	22.2* (1.99%)	0.58* (3.65%)	-
DPT1_F50	28.5	77.0	20.8	0.56	D
DPT2_F50	28.9	78.1	21.1	0.47	D
DPT3_F50	28.6	77.4	20.9	0.57	D
DPT_F50	28.7* (0.69%)	77.5* (0.69%)	21.0* (0.69%)	0.53* (10.37%)	-

Notes: *Average values of the S1 series; D = Debonding at adhesive/laminate interface; the values between parentheses are the corresponding coefficients of variation.

Table 3 — Main results obtained in the slabs: reference, pre- and post-fatigue tests.

Specimen ID	**Crack initiation**		**Yielding**		**Ultimate**		$\varepsilon_{max,CFRP}$ [%]	**FM**
	δ_{cr} [mm]	F_{cr} [kN]	δ_y [mm]	F_y kN]	δ_{max} [mm]	F_p [kN]		
SL_UN_M	1.03	2.6	25.11	11.4	52.80	12.0	-	CC
SL_STR_M	1.47	3.9	32.92	21.0	86.30	31.6	1.24	CC
SL_UN_F75	0.94*	2.8*	17.67	11.9	49.09	12.4	-	CC
SL_STR_F50	1.02*	3.0*	25.7	21.1	83.87	34.3	1.28	CC
SL_STR_F70	1.25*	3.6*	27.90*	19.4*	75.08	34.1	1.16	CC
SL_STR_F80	1.59*	3.4*	31.90*	20.4*	63.74	34.6	1.20	CC

Notes: *Pre-fatigue tests; CC – Concrete crushing.

Table 4 — Evolution of midspan deflection and stiffness during fatigue loading.

N_c	Level	SL_UN_F75		SL_STR_F50		SL_STR_F70		SL_STR_F80	
		δ [mm]	K [kN/mm]	δ [mm]	K [kN/mm]	δ [mm]	K [kN/mm]	δ [mm]	K [kN/mm]
1	S_{min}	20.40	0.86	19.16	0.96	42.42	0.86	53.22	0.79
	S_{max}	22.10		21.03		45.57		57.15)	
2,000,000	S_{min}	24.84 (8.3%)	0.81 (-5.7%)	26.6 (9.8%)	0.91 (-4.8%)	49.43 (7.4%)	0.84 (-2.1%)	61.49 (7.4%)	0.82 (3.6%)
	S_{max}	26.81 (7.9%)		28.35 (6.6%)		52.58 (6.4%)		65.21 (6.0%)	

Note: the values between parentheses are the variation of the parameter in comparison with the value obtained in the first cycle.

Table 5 — Strains (in percentage) attained on the first and last fatigue cycles at the midspan section.

Material	Cycle	Fatigue level	SL_STR_F50	SL_STR_F70	SL_STR_F80
CFRP – SG5	1	S_{min}	0.29	0.71	0.86
	2,000,000		0.30 (5.5%)	0.76 (6.6%)	0.90 (4.2%)
	1	S_{max}	0.44	0.83	1.0
	2,000,000		0.46 (4.7%)	0.88 (5.2%)	1.04 (3.3%)
Top concrete fiber	1	S_{min}	-0.066	-0.043	-0.22
	2,000,000		-0.030 (55.2%)	-0.011 (74.5%)	-0.16 (26.3%)
	1	S_{max}	-0.11	-0.087	-0.33
	2,000,000		-0.070 (36.0%)	-0.052 (40.7%)	-0.28 (17.1%)
Bottom steel – SG6	1	S_{min}	0.25	0.50	0.72
	2,000,000		0.26 (4.8%)	0.42 (-14.5%)	0.76 (5.3%)
	1	S_{max}	0.35	0.58	0.80
	2,000,000		0.37 (4.3%)	0.51 (-11.2%)	0.81 (1.0%)

Note: SG – Strain gauge; the values between parenthesis are the increase of strain from the first to the last fatigue cycle.

List of Figures

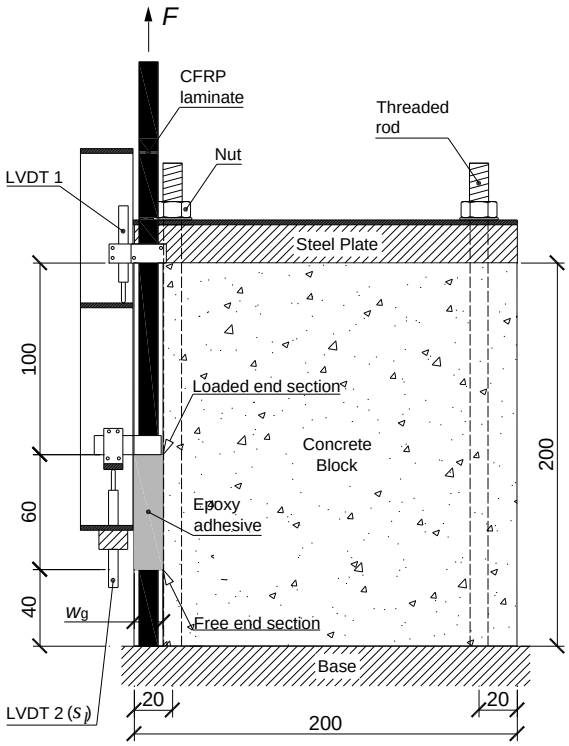

Figure 1 — Direct pullout tests: specimen geometry and test configuration. Note: all units are in millimeters.

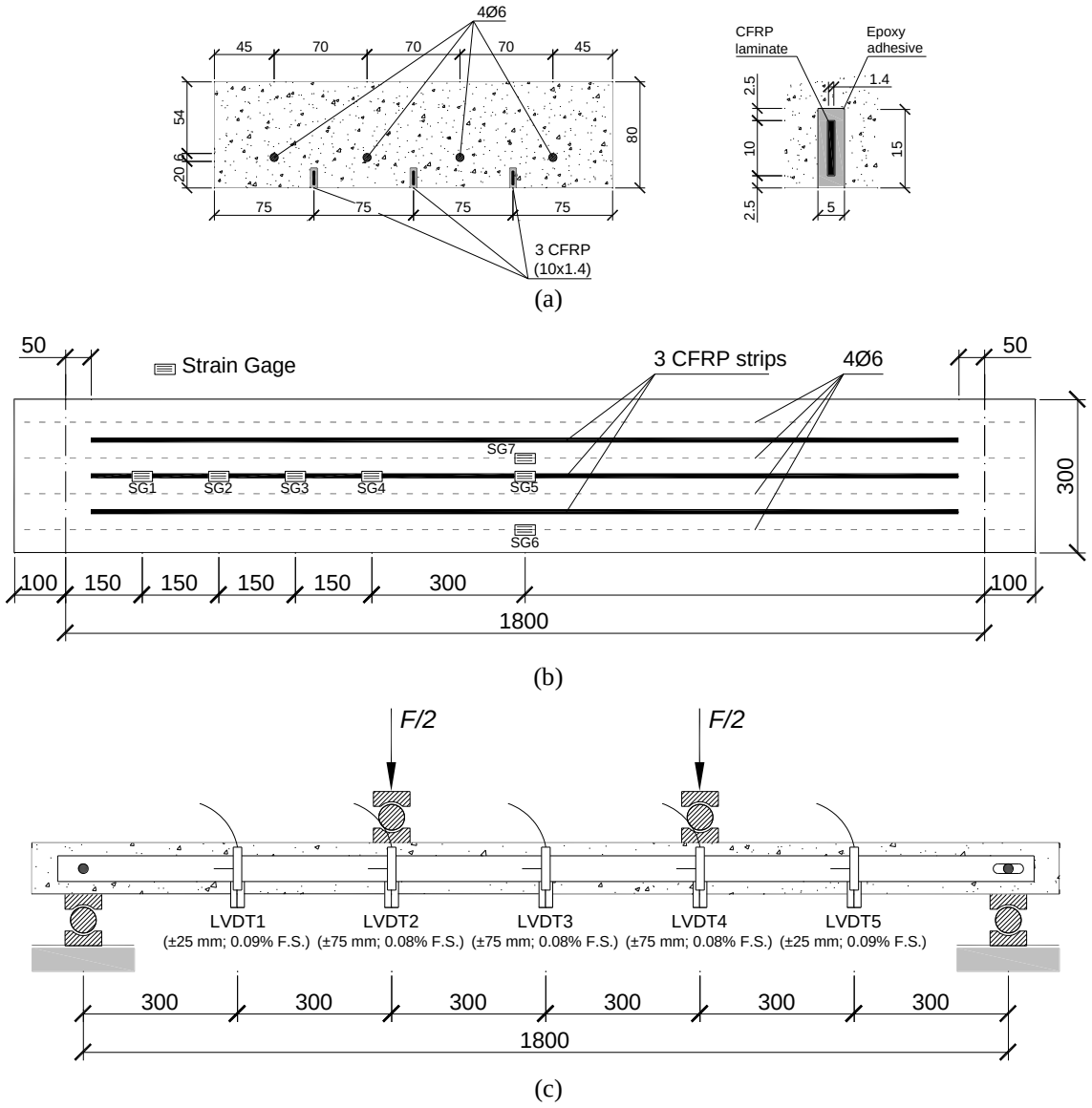

Figure 2 — Slab specimens: (a) Cross-section geometry and reinforcement detailing; (b) Longitudinal geometry, reinforcement detailing and gauge instrumentation; (c) Test configuration. Note: all units are in millimeters.

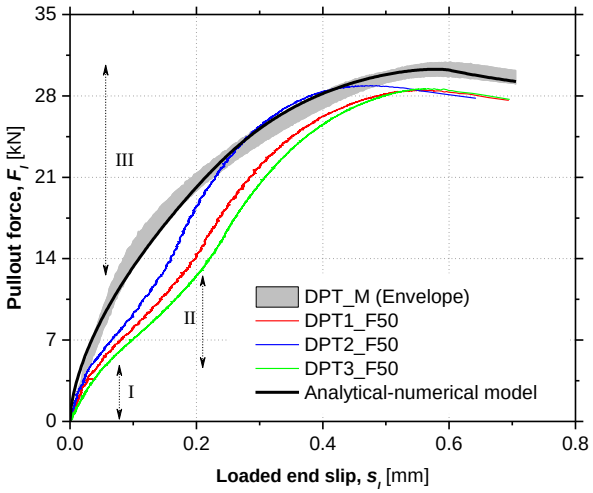

Figure 3 — F_l-s_l experimental responses for the series S1 and S2 under monotonic loading and numerical inverse analysis.

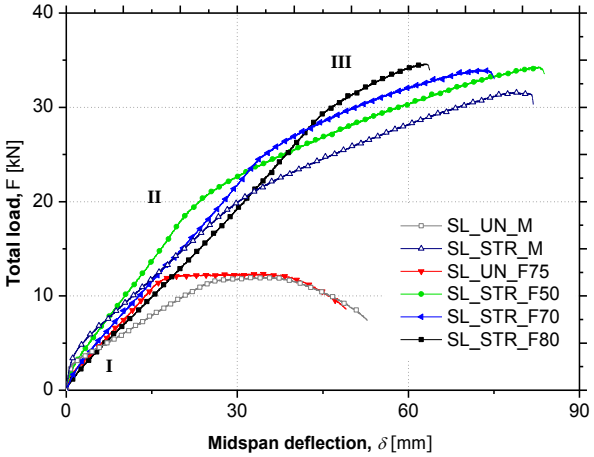

Figure 4 — Relationship between total load and midspan deflection of the reference tests and post-fatigue monotonic tests.

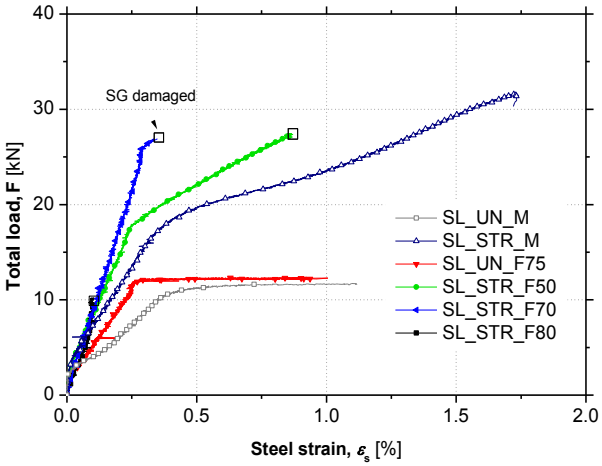

Figure 5 — Total load *versus* steel strain at midspan.

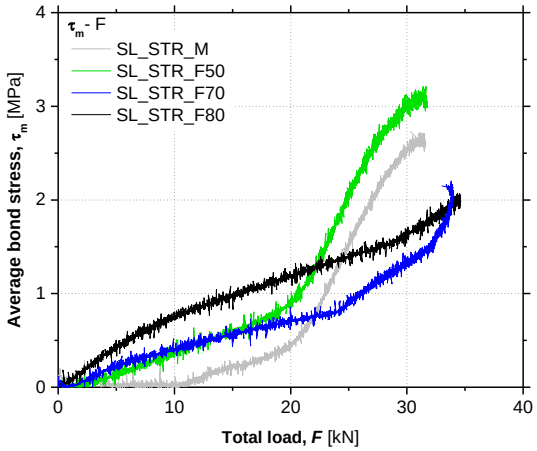

Figure 6 — Average bond stress and midspan deflection *versus* total load.

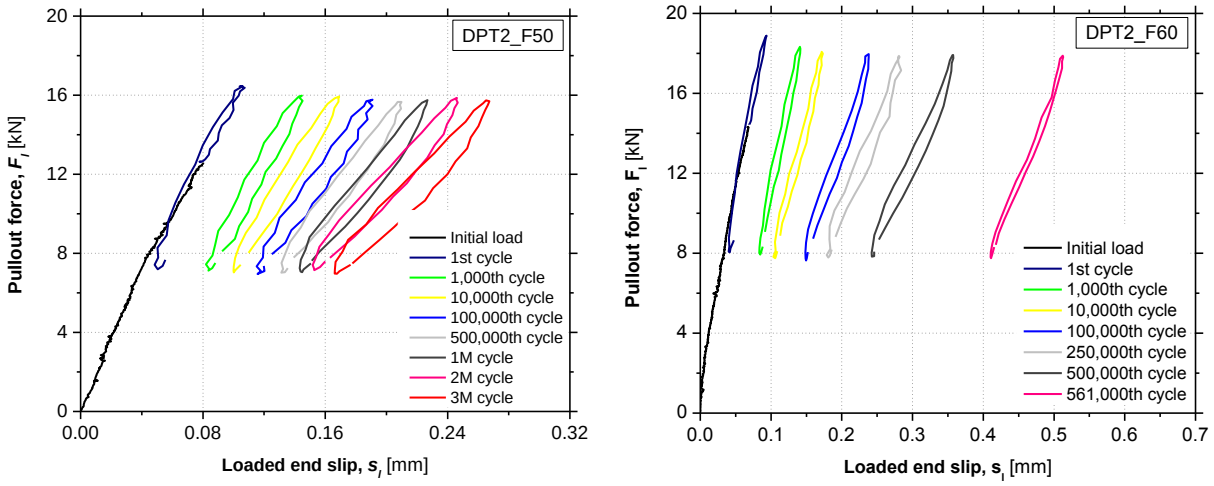

Figure 7 — Typical pullout force *versus* loaded end slip response during fatigue test: (a) DPT2_F50; (b) DPT2_F60.

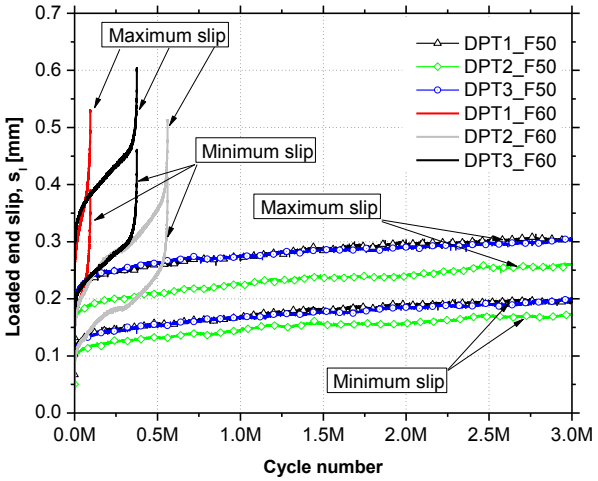

Figure 8 — Loaded end slip *versus* number of cycles.

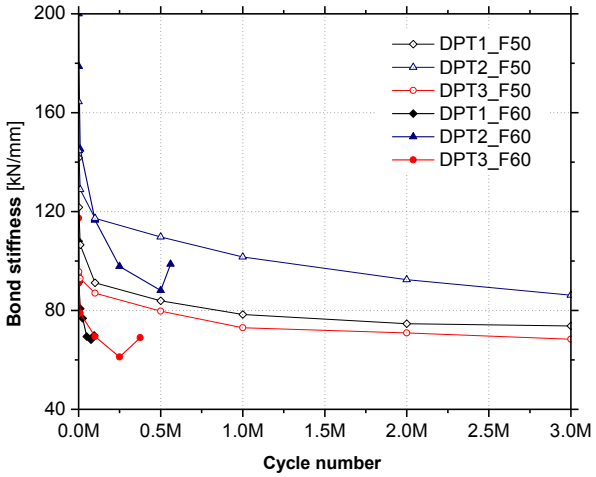

Figure 9 — Bond stiffness degradation along the cycles.

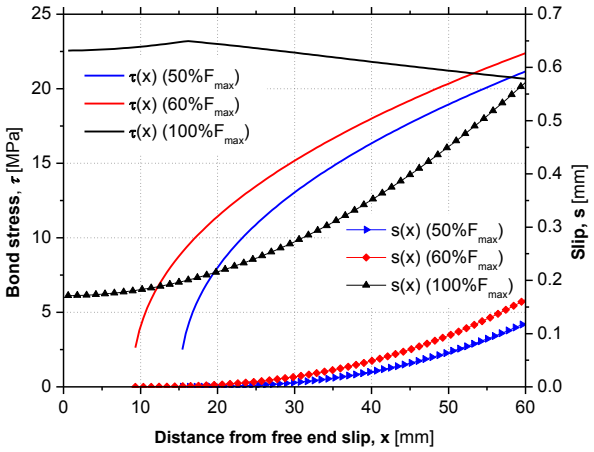

Figure 10 — Evolution of the bond stress, τ, and slip, s, along the CFRP longitudinal embedded length (x) for the 50%, 60% and 100% of the maximum pullout force.

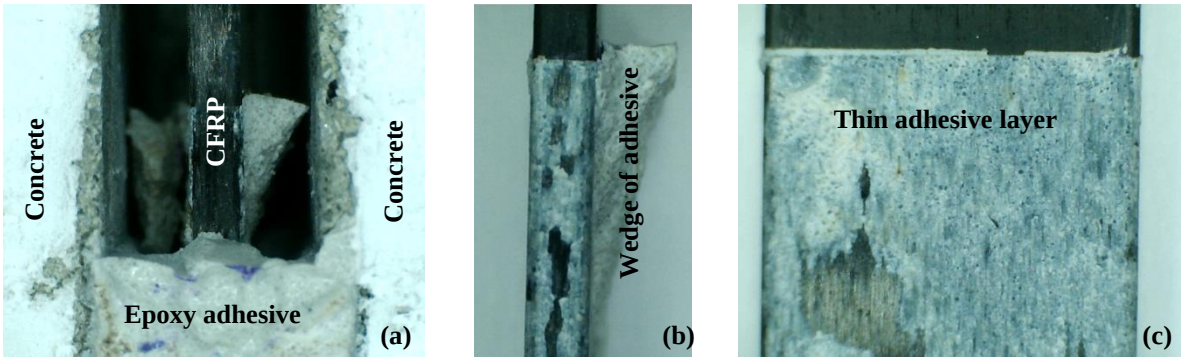

Figure 11 — Debonding failure at adhesive/laminate interface (20 times amplification): (a) detail of the debonding observed in monotonic tests at loaded end section (series S1); (b) and (c) fully debonding observed in series S3 – top and lateral view of the CFRP laminate, respectively.

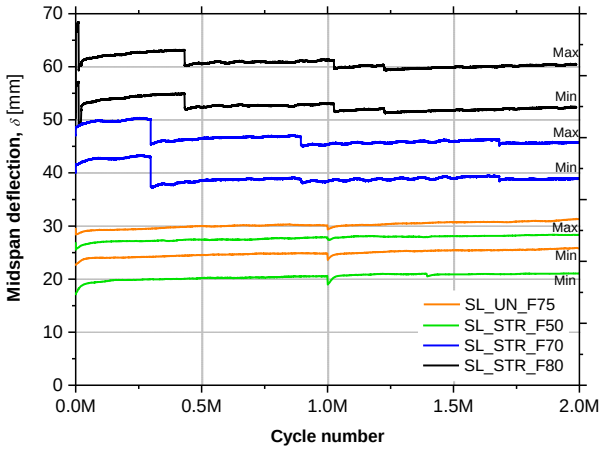

Figure 12 — Relationship between midspan deflection and cycle number of all slabs during fatigue test.

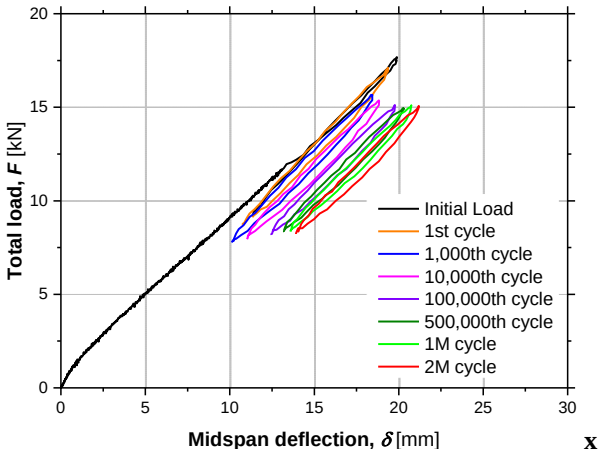

Figure 13 — Relationship between total load and midspan deflection of slab SL_STR_F50 during fatigue test.

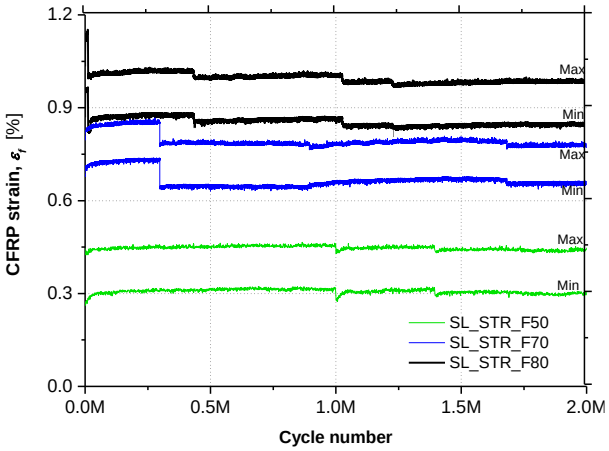

Figure 14 — Relationship between CFRP strain and cycle number of strengthened slabs during fatigue test.

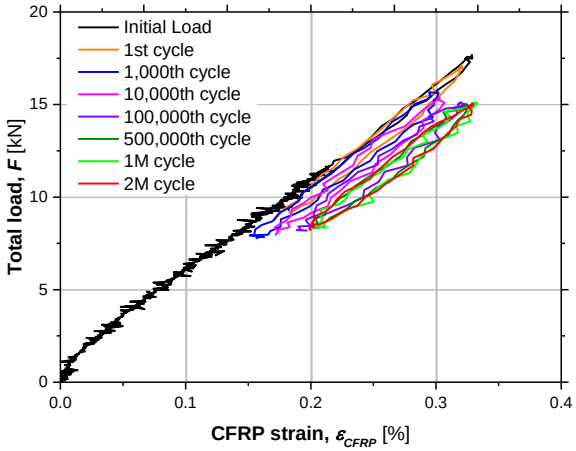

Figure 15 — Total load *versus* CFRP strain response of slab SL_STR_F70 during fatigue test.

NOTATION

The following symbols and acronyms are used in this paper:

CFRP: Carbon Fiber Reinforced Polymer

FRP: Fiber Reinforced Polymers

NSM: Near-Surface Mounted

EBR: Externally Bonded Reinforcement

RC: Reinforced Concrete

DPT: Direct Pullout Test

SL: Slab Specimen

S_{min}: minimum stress level

S_{max}: maximum stress level

F_{min}: minimum load of a fatigue cycle

F_{max}: maximum load of a fatigue cycle

F_p: maximum load carrying capacity

R: fatigue ratio

N_c: number of cycles that a specimen was submitted

STR: strengthened specimen

UN: unstrengthened specimen

s_l: loaded-end slip

F: applied load

$F_{f\max}$: maximum pullout force

F_{fu}: CFRP tensile strength

$s_{l\max}$: slip at the loaded end at $F_{f\max}$

$\tau_{\max,av}$: average bond strength at the CFRP-epoxy interface at $F_{f\max}$

P_f : perimeter of the CFRP cross-section in contact with the adhesive

L_b: bond length

ρ_l: longitudinal reinforcement ratio

$\rho_{s,eq}$: equivalent longitudinal reinforcement ratio

δ: midspan deflection

δ_{cr}: midspan deflection for crack initiation

F_{cr}: applied load for crack initiation

δ_{y}: midspan deflection for yield initiation of the longitudinal reinforcements

F_{y}: applied load for yield initiation of the longitudinal reinforcements

δ_{max}: midspan deflection for maximum load

L^{ij} : the distance between two consecutive strain gauges

τ_m^{ij} : average bond stress between two consecutive strain gauges

$\Delta\varepsilon_f^{ij}$: axial strain variation of strain gauges positioned at *i* and *j* sections

E_f: CFRP Young's modulus

A_f: cross-section area of the CFRP

K: stiffness

SG: Strain Gauge

CoV: Coefficient of Variation

LVDT: Linear Variable Differential Transducer